Received: 29 June 2021 | Accepted: 5 July 2021

DOI: 10.1002/mdp2.261

LETTER

WILEY

On the significance of diffuse crack width self-evolution in the phase-field model for residually stressed brittle materials

Enrico Salvati[1] | **Francesco Menegatti**[1] | **Manish Kumar**[1] | **Marco Pelegatti**[2] | **Alessandro Tognan**[1]

[1]Polytechnic Department of Engineering and Architecture (DPIA), University of Udine, Udine, Italy

[2]Department of Engineering, University of Ferrara, Ferrara, Italy

Correspondence
Enrico Salvati, Polytechnic Department of Engineering and Architecture (DPIA), University of Udine, Via delle Scienze 208. Udine 33100, Italy.
Email: enrico.salvati@uniud.it

Funding information
European Social Fund

Abstract

The Phase-Field method is an attractive numerical technique to simulate fracture propagation in materials relying on Finite Element Method. Its peculiar diffuse representation of cracks makes it suitable for a myriad of problems, especially those involving multiple physics and complex-shaped crack patterns.

Recent literature provided linear relationships between the width of the diffuse crack and the material intrinsic fracture toughness, through a material characteristic length. However, lately, it was shown how the existence of a residual stress field can affect the represented crack width even for fully homogeneous materials, in terms of toughness.

In this short note, the authors tried to shed some light on the factors influencing the width of the diffuse crack representation. By simulating crack propagation in several residually stressed brittle materials, it was shown how the width of the diffuse crack is affected by the ratio between the driving force - due to the externally applied load - and the driving force required to propagate the crack. In other words, the diffuse crack extent can be linked to the degree of crack propagation stability/instability. Monitoring the evolution of the studied quantity can be of great interest to rapidly assess crack instability circumstances, under displacement control.

KEYWORDS

J-resistance curve, finite element, fracture mechanics, residual stress, resistance curve, toughness

1 | INTRODUCTION

Modern structural mechanical design criteria rely more and more on damage-tolerant approaches.[1] This methodology is motivated by the need to put into service engineering systems that manifest first signs of failure well in advance, so that either safety or maintenance measures can be carried out before catastrophic or irreversible failures occur.

For this reason, in recent years, a considerable amount of effort has been put by the scientific community into the development of reliable tools to predict crack initiation and propagation in structures and materials. One of the most promising Finite Element Method (FEM)-based numerical technique, used to face this problem is called Phase-Field (PF) approach.[2,3] PF method employs a diffuse representation of cracks in a solid body, using a phase-field variable which assumes unitary value when the body is fully cracked and a null value when the material is in its pristine conditions, while a gradual transition between the two states is guaranteed. There exist a variety of FEM-based approach to tackle fracture mechanics problems, such as XFEM[4–6] or node release,[7] however, PF stands out for its performance when dealing with multi-physics problems,[8] crack branching/intersecting[9] and material nonlinearity.[2,10–14] In some instances, PF may be computationally costly, and for this reason, lately several strategies have been proposed.[15,16]

A very recent work proposed by one of the authors of the present paper combined - for the first time - the eigenstrain theory[17,18] within the PF framework to account for residual stress fields.[19–22] In that study, a single inclusion undergoing inelastic deformation (eigenstrain) was introduced in a Single Edge Notched Plate (SENP), assuming a homogeneous linear elastic and brittle material. It was shown how the presence of residual stress can affect the resistance curve of the material (R-curve), and thus how residual stress, if appropriately design, can be thought of as a material toughening mechanism. Interestingly, it was observed that the transverse width – with respect to the crack path - of the smeared crack representation is affected by the residual stress field.

In the present paper, the authors attempt to shed some light on the existence of a correlation between the diffuse crack representation width (Phase-Field Width, PFW) and the crack propagation behaviour in a monotonic loading context. Different sample configurations were employed including the presence of an inclusion subjected to a hydrostatic eigenstrain assuming several magnitudes spanning from positive to negative values. For these studied cases, the size of the PFW was monitored, and its evolution was compared to the R-curves obtained in a previous study reported in the literature.[19] The results are comprehensively discussed, and a sound explanation of the phenomena is provided.

2 | METHOD

A similar model discussed in detail in one of the author's recent publication[19] was employed in the present study. Both sample geometry and material properties were kept the same. In brief, the PF model proposed by Miehe[23] was used, with a history variable in the source term for the phase-field equation to account for the crack irreversibility, and the split of the elastic energy into tensile and compressive parts based on the spectral decomposition of the strain tensor into a compressive part and its tensile counterpart. This strain decomposition allowed for the introduction of an anisotropic model to ensure that crack propagates only under the effect of tensile deformation.[23] Moreover, both the geometric crack function and the energetic degradation function were of a quadratic form. Eigenstrain source was introduced by subtraction from the total strain in order to obtain the elastic strain tensor.

The SENP sample studied in the present analysis is shown in Figure 1, alongside other geometrical features, such as inclusion coordinates and size, and material properties in the corresponding table. In this study,"a" denotes the entire

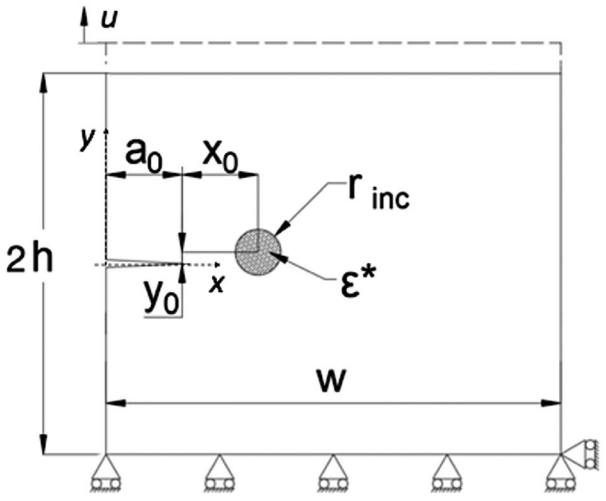

Dimension / Parameter	Description	Value
w	Sample width	120 mm
h	Half sample height	50 mm
a_0	Pre-crack length	20 mm
x_0	Inclusion centre x-coordinate	variable
y_0	Inclusion centre y-coordinate	variable
r_{inc}	Inclusion radius	6 mm
ε^*	Eigenstrain magnitude	variable
u	Imposed displacement of the sample upper end	variable over pseudo-time t
l_0	PF characteristic length	1 mm
E	Young's modulus	70 GPa
ν	Poisson's ratio	0.3
G_c	Fracture Toughness	4096 N/m

FIGURE 1 Sample geometry, boundary conditions and other parameters. Description of parameters and values given in the table

crack length, evaluated from the origin of the cartesian coordinate system shown in Figure 1, therefore by also including the pre-crack length (a_0). The employed material was of a linear elastic homogeneous type, under plane stress condition. The domain was discretised using adequate mesh refinement in correspondence of the envisaged crack propagation path.

3 | ANALYSIS & RESULTS

The study of the diffuse crack width was performed in two different inclusion configurations: a) $x_0 = 6\ mm$, $y_0 = 0\ mm$; b) $x_0 = 20\ mm$, $y_0 = 3\ mm$. For all these configurations, three different hydrostatic eigenstrain magnitudes were applied within the inclusion, i.e. $\varepsilon^* = -0.0015$, $\varepsilon^* = 0.0015$ and $\varepsilon^* = 0.0030$, in addition to the reference configuration: fully homogeneous material.

Given that the geometric crack function used in this work was of quadratic type,[24,25] this leads to a diffuse representation of the crack obeying the following function:

$$\emptyset = e^{-\frac{|\xi|}{l_0^*}} \tag{1}$$

Where $\emptyset$ is the crack PF, ξ is the diffuse crack transverse coordinate (according to Figure 1) and l_0^* is the parameter that identifies the width of the diffuse crack representation (PFW) – see Figure 2. Therefore, this function will be used to fit the results of the FEM simulation through the whole x-direction range. It is clear that the sought parameter is l_0^* and its evolution along x. This fitting procedure is applied at each extracted PF profile, once the crack has fully propagated. It is important to remind that this procedure is carried out by considering the undeformed configuration of the sample.

Once the value of the crack width has been estimated for each geometric and eigenstrain configuration (l^*_{0,ε^*}), the obtained profiles are normalised by the corresponding values for the simulation that does not consider the inclusion presence ($l^*_{0,\varepsilon^*=0}$), therefore a normalised crack width profile can be obtained:

$$\beta\,(x/w) = \frac{l^*_{0,\varepsilon^*}(x/w)}{l^*_{0,\varepsilon^*=0}(x/w)} \tag{2}$$

The result of the diffuse crack representation is reported in Figure 3(B), alongside the corresponding J-R curves (Figure 3(A)) to facilitate comprehension. It is clearly visible that the presence of a residually stressed field affects the width of the PF, indeed, β does not show a constant unitary value.

In principle, J-R curves provide a picture of the material fracture toughness as the crack progresses. Given the brittle nature of the analysed material, the actual J-R curves could not be evaluated within the regions where the externally applied load introduced a driving force exceeding the toughness of the material, i.e. crack instability. If the material

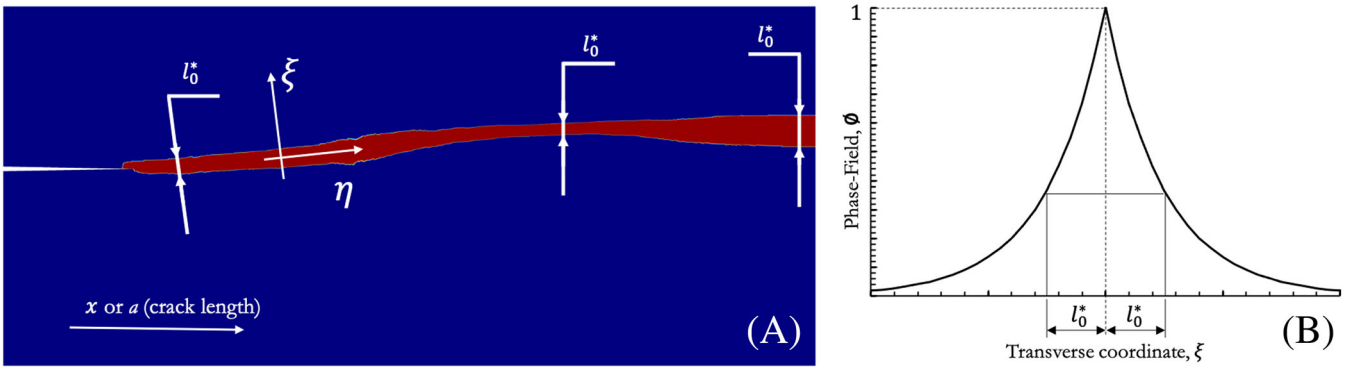

FIGURE 2 Crack smeared representation. (A) Filtered contour plot of phase-field representing a propagated crack and relevant dimensions and coordinates. (B) Crack representation profile using the quadratic geometric function representation and characteristic size l_0*

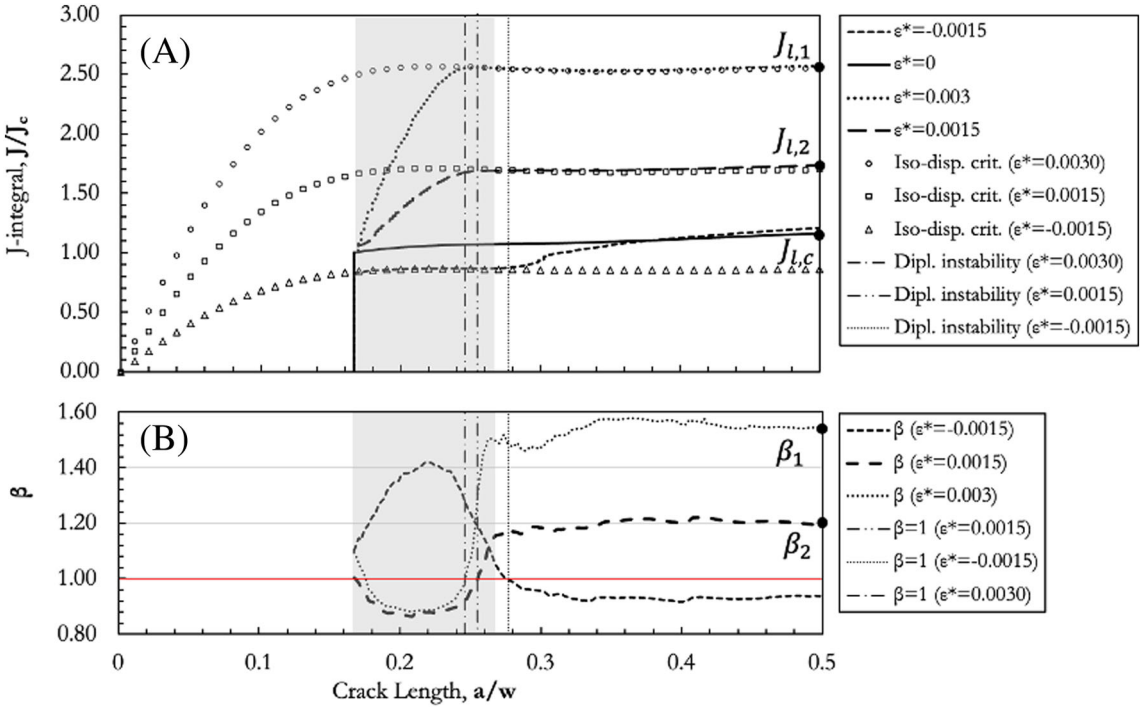

FIGURE 3 Results for the geometrical configuration $x_0 = 6\,mm$ & $y_o = 0$ at different hydrostatic eigenstrain in magnitudes. (A) J-R curves and (B) relative PF width as the crack propagates (shaded in grey the region occupied by the inclusion)

had shown a certain degree of ductility or some additional toughening contribution, then the sample could be partially and stably unloaded as the crack advanced, and the actual J-R curve could be evaluated. It is therefore evident that precise evaluation of J-R curves in brittle materials is a difficult task, particularly concerning experimental analyses. Nonetheless, the normalised PFW (β) can provide some insights on the difference between the externally applied driving force and the necessary driving force to allow for crack propagation.

For instance, if we consider the sample configuration devising an inclusion in correspondence of the pre-crack tip and a positive eigenstrain prescribed in it, the profile of β tells us something interesting. By neglecting the very first increase of the normalised PFW which is due to tensile stress generated at the crack tip by the inherent presence of the inclusion, it is visible how β decreases assuming values smaller than the unity. Within the range where $\beta < 1$, the presence of residual stress affected the J-R curve in a way that a pronounced material toughening is experienced, i.e. "rising" curve. Interestingly, at the crack length where $\beta = 1$, the propagating crack - under displacement control - reaches the instability condition, net of some numerical errors. The plots reported in Figure 3 come together with three different vertical lines that help to visualise the points crossing the $\beta = 1$ value and help to correlate these positions, in terms of *a/w*, with the iso-displacement curves intersecting the corresponding J-R curves (Figure 3(A)).

Once the displacement-control instability is reached, the applied driving force becomes gradually higher than the minimum driving force required to propagate the crack. Certainly, upon propagation of the crack past the inclusion the residual stress is fully relaxed and the material in this region must assume that the fracture toughness of the parent materials. So, in principle, the R-curve must fall and match the fully homogeneous residual stress-free toughness. However, as the externally applied load is monotonically increasing, this characteristic falling R-curve is not perceivable, and the external driving force is constantly higher than the material toughness. This aspect is noticeable by simply looking at the β profile that, depending on the applied driving force when the crack propagation instability is reached, assumes a nearly constant value. Hence, it is sensible to state that the PFW is somehow correlated with the ratio between the instantaneously applied driving force J_I and the actual fracture toughness $J_{I,C}$:

$$\lambda(x/w) = \frac{J_I(x/w)}{J_{I,C}(x/w)} \tag{3}$$

Both, the positive eigenstrain magnitudes analyses here confirm this trend. On the other hand, if a negative eigenstrain is imposed in the inclusion domain, then the generated tensile residual stress in this region will facilitate the propagation, making the crack propagation unstable as soon as the crack nucleates. As depicted in Figure 3(A), the iso-displacement curve associated with the displacement required to nucleate the crack at $\varepsilon^* = -0.0015$, makes the crack propagating in an unstable manner throughout the whole inclusion domain. Only after the crack has past the inclusion then the external driving force can be increased to make sure further propagation takes place. According to the observations made for the positive eigenstrain in the inclusion, the same conclusions can be drawn here. More explicitly, if $\beta > 1$ the crack propagates in an unstable manner, while as soon as β equates the unity, then the propagation that follows turns stable. It is worth reminding that these considerations are valid in theory, while in practical applications some other conditions need to be satisfied in order to arrest a crack that propagates in an unstable manner.[26]

The last remark is due to the $\beta < 1$ after passing the inclusion region for the $\varepsilon^* = -0.0015$ configuration. In this region, the crack overcomes the inclusion in a favourable way (given the tensile residual stress of the inclusion) and therefore it enters an unaffected domain of material where the crack driving force required to further propagation is higher than the current, therefore the crack propagates in a stable manner by gradually increasing the applied external displacement.

To obtain a further confirmation of the relationship between the PFW (β) and the ratio between the applied driving force and the local fracture toughness (λ), a second case-study was analysed. This concerned an inclusion centred at $x_0 = 20$ mm and $y_0 = 3$ mm, according to the coordinates depicted in Figure 1. Similarly, to what extracted from the previous case-study, the β profile was evaluated by monitoring the PFW and performing a normalisation with respect to the sample not showing the inclusion (fully homogeneous). The results are shown in Figure 4.

As well as the previous case, vertical lines were drawn to at the points where β turns its magnitude to values greater than the unity ($\beta > 1$); this is evident for those cases that considered positive eigenstrain magnitudes. Indeed, the same correspondence to the instability points under displacement control was found. In other words, when the iso-displacement curves intersect the J-R curves (Figure 4(A)), β crosses the unity level (horizontal line in red). Remarkably, before the crack entered the inclusion, the negative eigenstrain hydrostatic case showed relatively low β values (mostly below 1), meaning that the compressive residual stress in front of the crack tip reinforced the stable crack propagation condition, at least under displacement-controlled load. Nevertheless, it is worth highlighting the numerical errors within this region can play a relevant role and therefore these conclusions may be affected by an insufficient

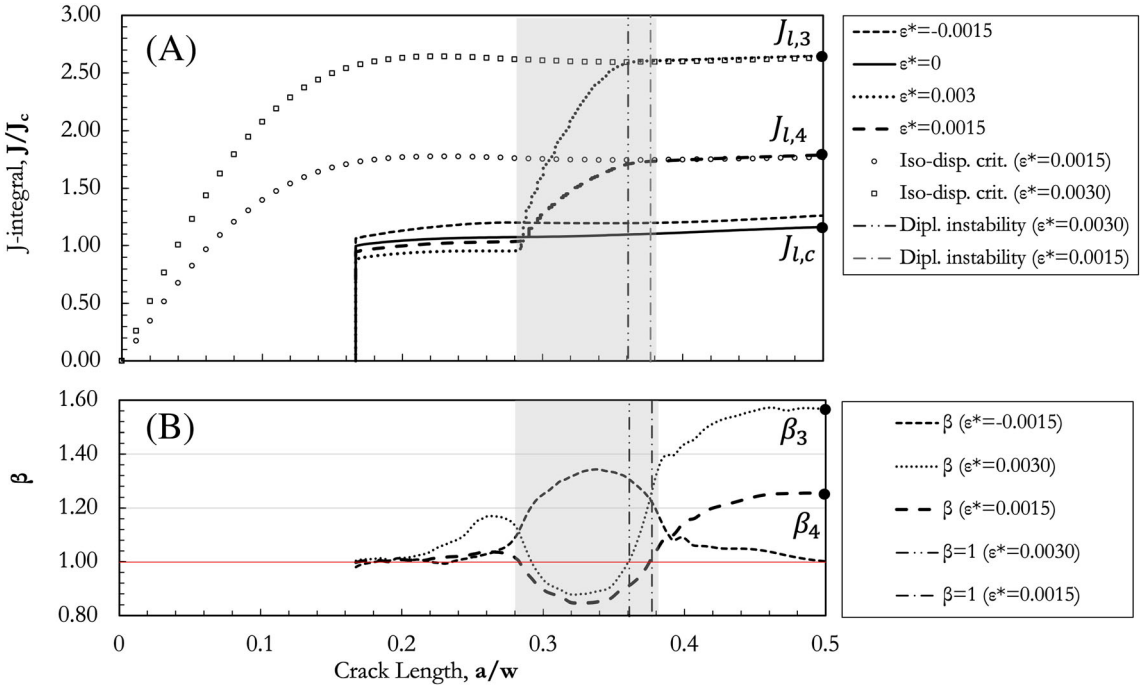

FIGURE 4 Results for the geometrical configuration $x_0 = 20\,mm$ & $y_0 = 3\,mm$ at different hydrostatic eigenstrain in magnitudes. (A) J-R curves and (B) relative PF width as the crack propagates (shaded in grey the region occupied by the inclusion)

statistical correlation. Lastly, as expected, but not strikingly noticeable as the previously obtained J-R curves, the negative eigenstrain (tensile residual stress within the inclusion) generated an increase of β, meaning that the fracture toughness within the inclusion resulted to be lower than the surrounding and therefore crack propagation instability occurred.

A correlation analysis was performed to verify that the hypothesis of a close relationship, between the PFW (β) and the crack driving force ratio (λ), does exist. The correlation coefficient was estimated through the analysis of the positive eigenstrain case-studies at crack propagation length of $a/w = 0.5$. By considering the local values of J-integral at $a/w = 0.5$, as indicated by the filled circles in both Figure 3 and Figure 4, local values of λ_i were found. At the same crack extent, values of PFW were extracted as well (β_i). The crack propagation length of $a/w = 0.5$ was chosen because at this propagation stage the crack has overcome the inclusion (no residual stress presence) and therefore the actual material toughness is well-known to be the intrinsic material toughness.

Correlation between β_i and λ_i was found to be high enough to confirm the hypothesis, i.e. 0.9915. Thereby, it can be inferred that β provides information about the actual material fracture toughness with respect to the externally applied force.

A simple empirical power-law relationship could be found to link together the β and λ:

$$\lambda = \beta^m \tag{4}$$

where m is an empirical coefficient that turned out to be 1.8 for the case reported in the present study, giving rise to relative errors smaller than 7%. However, some factors might affect the link between the two parameters, for instance the type of PF formulation. Eventually, further effort is still required to generalise the findings of this study.

4 | CONCLUSIONS

The analysis presented in this study showed how information regarding crack propagation stability can be extracted from the Phase-Field method. In particular, the significance of the variation of the Phase-Field diffuse zone width (PFW) during crack propagation has been revealed for residually stressed brittle materials. A causal link between the ratio of externally applied to necessary crack propagation driving forces and the corresponding PFW was found. Given that the determination of the actual R-curve becomes very challenging for brittle materials as it is extremely difficult to stop an unstably propagating crack, the PF method can help to identify local fracture toughness changes, at least when dealing with residually stressed materials.

A simple empirical formulation has been proposed to establish a mathematical relationship between the two analysed aspects. However, further effort should be made to establish a more rigorous relationship between the R-curves and the PFW, depending on a variety of PF crack diffuse representation ways proposed in the literature.

ACKNOWLEDGEMENTS

The authors would like to acknowledge the European Social Fund (ESF) for providing funds to support Dr. Manish Kumar.

DATA AVAILABILITY STATEMENT

The data that support the findings of this study are available on request from the corresponding author. The data are not publicly available due to privacy or ethical restrictions.

ORCID

Enrico Salvati https://orcid.org/0000-0002-2883-0538

REFERENCES

1. Ritchie RO. The conflicts between strength and toughness. *Nat Mater*. 2011;10(11):817-822.
2. Wu J-Y. A unified phase-field theory for the mechanics of damage and quasi-brittle failure. *J Mech Phys Solids*. 2017;103:72-99.
3. Francfort GA, Marigo JJ. Revisiting brittle fracture as an energy minimization problem. *J Mech Phys Solids*. 1998;46(8):1319-1342.
4. Fries TP, Belytschko T. The extended/generalized finite element method: An overview of the method and its applications. *Int J Numer Methods Eng*. 2010;84(3):253-304.

5. Kumar M, Singh IV. Numerical investigation of creep crack growth in plastically graded materials using C(t) and XFEM. *Eng Fract Mech*. 2020;226:106820. https://doi.org/10.1016/j.engfracmech.2019.106820
6. Kumar M, Singh IV, Mishra BK, Ahmad S, Rao AV, Kumar V. Mixed mode crack growth in elasto-plastic-creeping solids using XFEM. *Eng Fract Mech*. 2018;199:489-517.
7. Materna A, Oliva V. Elastic-plastic FEM investigation of the thickness effect on fatigue crack growth. *Procedia Eng*. 2011;10:1109-1114.
8. Martínez-Pañeda E, Golahmar A, Niordson CF. A phase field formulation for hydrogen assisted cracking. *Comput Methods Appl Mech Eng*. 2018;342:742-761.
9. Carollo V, Reinoso J, Paggi M. Modeling complex crack paths in ceramic laminates: A novel variational framework combining the phase field method of fracture and the cohesive zone model. *J Eur Ceram Soc*. 2018;38(8):2994-3003.
10. Alessi R, Marigo J-J, Vidoli S. Gradient damage models coupled with plasticity: Variational formulation and main properties. *Mech Mater*. 2015;80:351-367.
11. Ulloa J, Wambacq J, Alessi R, Degrande G, François S. Phase-field modeling of fatigue coupled to cyclic plasticity in an energetic formulation. *Comput Methods Appl Mech Eng*. 2021;373:113473. https://doi.org/10.1016/j.cma.2020.113473
12. Lancioni G, Alessi R. Modeling micro-cracking and failure in short fiber-reinforced composites. *J Mech Phys Solids*. 2020;137:103854. https://doi.org/10.1016/j.jmps.2019.103854
13. Alessi R, Crismale V, Orlando G. Fatigue Effects in Elastic Materials with Variational Damage Models: A Vanishing Viscosity Approach. *Int J Nonlinear Sci*. 2019;29(3):1041-1094.
14. Alessi R, Freddi F, Mingazzi L. Phase-field numerical strategies for deviatoric driven fractures. *Comput Methods Appl Mech Eng*. 2020; 359:112651. https://doi.org/10.1016/j.cma.2019.112651
15. Hirshikesh EM, Natarajan S. Adaptive Phase Field Modelling of Crack Propagation in Orthotropic Functionally Graded Materials. *Def Technol*. 2021;17(1):185-195.
16. Kristensen PK, Martínez-Pañeda E. Phase field fracture modelling using quasi-Newton methods and a new adaptive step scheme. *Theor Appl Fract Mech*. 2020;107:102446. https://doi.org/10.1016/j.tafmec.2019.102446
17. Salvati E, Korsunsky AM. A Simplified FEM Eigenstrain Residual Stress Reconstruction for Surface Treatments in Arbitrary 3D Geometries. *Int J Mech Sci*. 2018;138-139:457-466.
18. Korsunsky AM. *A Teaching Essay on Residual Stresses and Eigenstrains*. Elsevier Inc; 2017.
19. Salvati E. Residual Stress as a Fracture Toughening Mechanism: A Phase-Field Study on a Brittle Material. *Theor Appl Fract Mech*. 2021; 114:103021. https://doi.org/10.1016/j.tafmec.2021.103021
20. Salvati E, Lunt AJG, Heason CP, Baxter GJ, Korsunsky AM. An analysis of fatigue failure mechanisms in an additively manufactured and shot peened IN 718 nickel superalloy. *Mater Des*. 2020;191:108605. https://doi.org/10.1016/j.matdes.2020.108605
21. Salvati E, Korsunsky AM. An analysis of macro- and micro-scale residual stresses of Type I, II and III Using FIB-DIC Micro-Ring-Core Milling and Crystal Plasticity FE Modelling. *Int J Plast*. 2017;98:123-138.
22. Salvati E, Zhang H, Fong KS, Song X, Korsunsky AM. Separating plasticity-induced closure and residual stress contributions to fatigue crack retardation following an overload. *J Mech Phys Solids*. 2017;98:222-235.
23. Miehe C, Welschinger F, Hofacker M. Thermodynamically consistent phase-field models of fracture: Variational principles and multi-field FE implementations. *Int J Numer Methods Eng*. 2010;83(10):1273-1311.
24. Miehe C, Hofacker M, Welschinger F. A phase field model for rate-independent crack propagation: Robust algorithmic implementation based on operator splits. *Comput Methods Appl Mech Eng*. 2010;199(45):2765-2778.
25. Bourdin B, Francfort GA, Marigo JJ. Numerical experiments in revisited brittle fracture. *J Mech Phys Solids*. 2000;48(4):797-826.
26. Xu W, Wintle JB, Wiesner CS, Turner DG. Analysis of crack arrest event in NESC-1 spinning cylinder experiment. *Int J Press Vessel Pip*. 2002;79(11):777-787.

How to cite this article: Salvati E, Menegatti F, Kumar M, Pelegatti M, Tognan A. On the significance of diffuse crack width self-evolution in the phase-field model for residually stressed brittle materials. *Mat Design Process Comm*. 2021;e261. https://doi.org/10.1002/mdp2.261